Spd2 assists Spd1 in modulation of RNR architecture but does not regulate deoxynucleotide pools

Article (Accepted Version)

Spd2 assists Spd1 in modulation of RNR architecture but does not regulate deoxynucleotide pools

Rasmus Vejrup-Hansen[1], Oliver Fleck[1,3], Katrine Landvad[1], Ulrik Fahnøe[1], Sebastian S. Broendum[1], Ann-Sofie Schreurs[2], Birthe B. Kragelund[1], Antony M. Carr[2], Christian Holmberg[1] and Olaf Nielsen[1,*]

[1] Department of Biology, University of Copenhagen, Ole Maaløes Vej 5, 2200 Copenhagen N., DK

[2] Genome Damage and Stability Centre, School of Life Sciences, University of Sussex, Falmer, Brighton, East Sussex BN1 9RQ, UK.

[3] NWCR Institute, School of Biological Sciences, Bangor University, Bangor, Gwynedd, LL57 2UW, UK

Running title: *spd2* in fission yeast

Keywords: genome stability, ribonucleotide reductase, CRL4^{Cdt2} ubiquitin ligase, intrinsically disordered proteins (IDPs), *S. pombe*, cancer model

*Correspondence should be addressed to: Olaf Nielsen, Department of Biology, University of Copenhagen, E-mail: onigen@bio.ku.dk

JCS Advance Online Article. Posted on 20 March 2014

Abstract

In yeasts, small intrinsically disordered proteins (IDPs) modulate ribonucleotide reductase (RNR) activity to ensure an optimal supply of dNTPs for DNA synthesis. The *S. pombe* Spd1 protein can directly inhibit the large RNR subunit (R1), import the small subunit (R2) into the nucleus and induce an architectural change in the R1-R2 holocomplex. Here, we report the characterization of Spd2, a protein with homology to Spd1. We show that Spd2 is a $CRL4^{Cdt2}$ controlled IDP that functions together with Spd1 in the DNA damage response and in modulation of RNR architecture. However, Spd2 does not regulate dNTP pools and R2 nuclear import. Furthermore, deletion of *spd2* only weakly suppresses the $Rad3^{ATR}$ checkpoint dependency of $CRL4^{Cdt2}$ mutants. However, when we raised intracellular dNTP pools by inactivation of RNR feedback inhibition, deletion of *spd2* could suppress the checkpoint dependency of $CRL4^{Cdt2}$ mutant cells to the same extent as *spd1*. Collectively, these observations suggest that Spd1 on its own regulates dNTP pools, while it together with Spd2 modulates RNR architecture and sensitizes cells to DNA damage.

Introduction

Correct regulation of DNA building block levels is emerging as a pre-requisite for the maintenance of genome integrity. Cancer development is presumed to be initiated by oncogenic mutations that cause replication stress, thereby increasing the risk of replication fork collapse and subsequent formation of DNA lesions (Halazonetis et al., 2008). This type of oncogenic replication stress has been reported to be accompanied by a significant reduction in cellular deoxynucleoside triphosphate (dNTP) pools, possibly due to an imbalance between nucleotide synthesis and DNA replication activity (Beck et al., 2012; Bester et al., 2011) . Furthermore, such oncogenic S phase problems, including shorter inter origin distances and slower fork migration, can be reversed by an exogenous supply of nucleosides, suggesting that insufficient levels of DNA building blocks may play an important causal role in early stages of tumour development.

The rate-limiting step in dNTP production is catalysed by the essential and highly conserved enzyme ribonucleotide reductase (RNR), which reduces ribonucleoside diphosphates to their corresponding deoxy forms. Eukaryotic cells utilize class 1a RNR, a heteromeric enzyme consisting of up to three copies of two different dimeric subunits, R1 and R2. The catalytic activity resides in the large R1 subunit, while the smaller R2 subunit donates reducing power to the reaction from a diferric tyrosyl radical (Nordlund and Reichard, 2006).

Consistent with deoxynucleotide pools being important for maintenance of genome integrity, cellular RNR function is tightly regulated at several levels. Expression of both subunits is induced under conditions where DNA synthesis is required, i. e. in S phase or after DNA damage (Elledge et al., 1993). Furthermore, the activity of RNR is regulated by two intricate feedback control mechanisms (Reichard, 2010). The R1 subunit contains two allosteric effector binding sites, the specificity site (S site) and the activity site (A site). The S site ensures a balanced supply of the four DNA building blocks, by binding dNDP species present in excess thereby remodeling the catalytic

site towards other base substrates. The A site represents a molecular switch that regulates the overall activity of the enzyme by monitoring the cellular dATP/ATP ratio: RNR is inactive when dATP is bound, and it becomes activated when dATP is replaced by ATP. Recent structural studies suggest that the inactive form of the enzyme is a hexameric ring consisting of three R1 dimers with an R2 dimer embedded in the middle (Fairman et al., 2011). Less is known about the structure of the active, ATP bound form, but the molecular interaction between the R1 and R2 subunits appears to be altered relative to the dATP bound complex, and it may contain additional R2 dimers (Hofer et al., 2012). RNR can be locked genetically in its active configuration by replacing Asp 57 in the A site with Asn. Mammalian cell lines harbouring this D57N mutated version of R1 have highly increased dNTP pools indicating that a large proportion of RNR complexes normally is in the inhibited form in vivo (Weinberg et al., 1981).

In yeasts, RNR activity is additionally regulated by a group of small intrinsically disordered proteins (IDPs). In fission yeast, the Spd1 protein can inhibit RNR by two different mechanisms. It can sequester the R2 subunit in the nucleus, away from the R1 subunit which is mainly cytosolic (Liu et al., 2003), and it can also directly bind to and inhibit the R1 subunit (Hakansson et al., 2006). We recently reported that Spd1 can modulate the RNR complex in yet a third fashion: If the R1 and R2 subunits are tagged with different fluorescent proteins, a fluorescence resonance energy transfer (FRET) reaction can be observed between them, and this signal is absent in *Δspd1* cells (Nestoras et al., 2010). It is unclear how the underlying Spd1-mediated change in the molecular interactions between R1 and R2 affects RNR function. Interestingly, these three molecular functions of Spd1 can be separated genetically, suggesting that the protein mediates them by different molecular mechanisms (Nestoras et al., 2010).

The limited sequence conservation of RNR inhibitory IDPs has thus far precluded resolving the issue of whether mammalian counterparts exist. However, in the distantly related budding yeast *S.*

cerevisiae, two Spd1-related IDPs, Dif1 and Sml1, sequester R2 in the nucleus or inhibit R1, respectively. Interestingly, synteny analysis suggests that these two genes arose through genome duplication of a common ancestor with both functions, similar to *S. pombe* Spd1 (Lee et al., 2008). A third potential Spd1-related protein, Hug1, is also predicted in the budding yeast genome, but no function has yet been assigned to this (Basrai et al., 1999).

When fission yeast cells undergo DNA replication or repair, the Spd1 protein becomes degraded by $CRL4^{Cdt2}$ mediated ubiquitylation (Holmberg et al., 2005; Liu et al., 2003), a process that is mediated on chromatin-associated PCNA (Salguero et al., 2012), and also requires the Csn1 and Csn2 subunits of the COP9/signalosome (Liu et al., 2003). The $CRL4^{Cdt2}$ E3 ubiquitin ligase is activated by transcriptional induction of the Cdt2 substrate adaptor, which becomes expressed in unperturbed S phase by the MCB transcription complex. Following DNA damage, Cdt2 is induced by a $Rad3^{ATR}$-dependent pathway (Liu et al., 2005; Moss et al., 2010).

$CRL4^{Cdt2}$ defective cells undergo DNA replication in the presence of Spd1, and this gives rise to severe S-phase stress: replication proceeds slowly, with concomitant activation of the $Rad3^{ATR}$ checkpoint, which becomes essential for cell survival under these conditions. Furthermore, such cells are hypersensitive to DNA damaging agents, are defective in double-strand break (DSB) repair by homologous recombination, display a more than 20 fold increase in spontaneous mutation rates, and are also completely unable to undergo pre-meiotic S phase (Holmberg et al., 2005; Liu et al., 2005; Liu et al., 2003; Moss et al., 2010). The requirement for a functional $Rad3^{ATR}$ pathway and the defects in recombination and pre-meiotic S-phase are all fully reversed by deletion of the *spd1* gene or by overexpression of fission yeast R2 ($Suc22^{R2}$), suggesting that these phenotypes are caused by Spd1-mediated RNR inhibition. On the other hand, the increased mutation rates and sensitivity to DNA damage are only partially suppressed by Spd1 loss, indicating that deregulation of other $CRL4^{Cdt2}$-controlled processes also contributes to these phenotypes.

The systematic genetic analysis of *spd1* has shown that certain mutants defective in nuclear import of the RNR R2 subunit or in the FRET reaction between R1 and R2 still require the $Rad3^{ATR}$ pathway for survival when the Spd1 degradation pathway is inactivated (Nestoras et al., 2010). These observations are consistent with a model where Spd1 causes checkpoint activation by inhibiting dNTP formation via direct binding to RNR. However, we recently reported that Spd1 accumulation can cause checkpoint activation even in cells that have highly elevated dNTP pools due to inactivation of RNR feedback inhibition (Fleck et al., 2013). Hence, Spd1 may also cause checkpoint activation independently of deoxynucleotide synthesis.

In the present study we have characterized Spd2, an Spd1-related putative RNR inhibitor that was identified in a comparative genome sequencing study (Rhind et al., 2011). We show that Spd2, similar to Spd1, is an IDP that becomes degraded by $CRL4^{Cdt2}$ ubiquitylation following inhibition of RNR by hydroxyurea. Similar to *Δspd1,* deletion of *spd2* can rescue the damage sensitivity of $CRL4^{Cdt2}$ mutants, and Spd2 - like Spd1 - is required for the FRET signal between R1 and R2. However, Spd2 does not share the ability of Spd1 to sequester the R2 subunit in the nucleus, and – surprisingly – it does not seem to affect cellular dNTP pools. These observations support a model where Spd2 can assist Spd1 in an S phase inhibitory pathway that functions independently of dNTP formation.

Results

Spd2 – a new RNR inhibitor homolog

The genomes of four *Schizosaccharomyces* species have recently been sequenced (Rhind et al., 2011). The availability of the sequences of three additional fission yeast species allowed the identification of more than 100 new conserved open reading frames in the *S. pombe* genome. One of these proteins, Spd2, shows limited homology to Spd1 (19% overall sequence identity) and other RNR inhibitors (Figure 1).

In general, the homology among RNR inhibitors is limited to a number of short motifs. The Spd1 and Spd2 orthologues also appear to have diverged considerably, but are very well conserved within the Spd1 and Spd2 subgroups (Figure 1A). The Spd1 and Spd2 families share a small domain near their C-terminal ends, which is absent in the other known RNR inhibitors. We will refer to this as the Spd domain (Figure 1B).

The Spd1 and Spd2 orthologues of the four fission yeast species all contain a Hug domain (Figure 1A), which is also present in the *S. cerevisiae* Hug1 and Dif1 proteins and in *Ashbya gossypii* Aer122c, but absent in budding yeast Sml1 (Figure 1B). The Hug domain of Dif1 is required for nuclear import of the small RNR subunit (Lee et al., 2008; Wu and Huang, 2008), and genetic analysis suggests that the Hug domain of Spd1 may have a similar function (Nestoras et al., 2010). The N-terminal part of the Hug domain in Spd1 was recently shown to constitute a PIP (PCNA interacting protein) degron, mediating binding to PCNA, which is a prerequisite for $CRL4^{Cdt2}$-dependent ubiquitylation and subsequent degradation of Spd1 (Salguero et al., 2012). This motif is present in Spd2 (Figure 1), suggesting that the protein is degraded by a similar mechanism (see below).

The $CRL4^{Cdt2}$ degradation pathway is absent in budding yeast. Instead, degradation of Sml1 and Dif1 during S phase or in response to DNA damage is triggered by Dun1-mediated phosphorylation

of a phospho-degron referred to as the Sml1 domain (Lee et al., 2008; Uchiki et al., 2004; Wu and Huang, 2008; Zhao and Rothstein, 2002). Consistent with a different degradation mechanism in fission yeast, this Sml1-degron is absent in both Spd1 and Spd2 (Figure 1B).

Finally, Sml1 can bind to and inhibit the large RNR subunit through its Rnr1 domain (Zhao et al., 2000). Although it has been shown that *S. pombe* Spd1 also can bind to the large RNR subunit (Hakansson et al., 2006), conservation of the Rnr1 domain in Spd1 is limited to a short stretch of amino acid residues. In Spd2, the homology to the Rnr1 domain is even more limited, if not absent (Figure 1B).

Spd2 is an intrinsically disordered protein

Similar to Spd1 and Sml1 (Danielsson et al., 2008; Nestoras et al., 2010), the sequence of Spd2 has the typical characteristics of an IDP: a high content of charged residues (29%) and a low aliphatic index (67.94; for reference, myoglobin = 95.1). These proteins lack well-structured three-dimensional folds and are distinctive by having regions that form lowly populated, transient structures and/or contain conserved sequence motifs (Tompa, 2002). Importantly, these local features are central to target recognition and the flexibility of the IDPs is essential for binding to more than one partner. To investigate the disorder characteristics of Spd2 by spectroscopy, recombinant Spd2 was produced in *E. coli* and purified to > 98% homogeneity (Figure 2A). A far-UV CD spectrum of Spd2 showed no signs of pronounced secondary structure elements, with little negative ellipticity in the 210-220 nm range (Figure 2B). Instead, a large negative ellipticity with maximum at 199 nm suggested a disordered protein with little or no secondary structure. In support of this, an $^{15}N,^{1}H$-HSQC NMR spectrum of ^{15}N-labeled Spd2 recorded at 10 °C showed a narrow dispersion of signals in the ^{1}H- dimension, further suggesting that the protein is disordered with no globular fold (Figure 2C). Unlike Spd1, the peaks of the NMR spectrum of Spd2 were of almost

equal intensity, revealing the higher solubility of this protein compared to Spd1 (Nestoras et al., 2010) and (data not shown). Thus, Spd2 possesses hallmarks of an IDP (Tompa, 2002) with low-complexity sequence, a lack of secondary structure elements in a far-UV CD spectrum and a collapsed NMR spectrum.

Spd1 and Spd2 both inhibit S phase

We next constructed a strain deleted for the *spd2* gene. Similarly to *Δspd1* cells, this Δ*spd2* strain showed no obvious phenotypic differences to wild type regarding cell shape and growth rate (data not shown). Spd1 was originally identified as a protein that inhibited S-phase progression when over-expressed, thereby causing cell elongation (Woollard et al., 1996). We found that overexpression of Spd2 similarly caused cell elongation (Figure 3A). Elongation of cells by overexpression of Spd2 did not require functional Spd1 and *vice versa*.

Next, we used flow cytometry (FACS) to monitor the cell-cycle distribution in cells overexpressing Spd1 or Spd2. Interpretation of FACS data in fission yeast is complicated by the fact that G1 and S phase cells are still attached to their sisters, thus giving rise to a 2C signal. However, by measuring the DNA signal width, it is possible to discriminate G1 and S cells from G2 cells (Knutsen et al., 2011), thus giving a more precise estimate of the S-phase population. By this method we found that overexpression of Spd2 caused a strong increase in the number of cells undergoing S phase, suggesting that the protein - similarly to Spd1 - delays DNA replication (Figure 3B + Suppl. Figure S1). Again, Spd1 and Spd2 could cause this phenotype independently of each other.

Spd2 is a CRL4^{Cdt2} target

Spd1 is a target of the CRL4^{Cdt2} E3 ubiquitin ligase (Holmberg et al., 2005; Liu et al., 2005; Liu et al., 2003), and we next investigated if this was also the case for Spd2. Since we found that epitope tagging of Spd1 adversely affected its functionality (data not shown), we raised antibodies against recombinant Spd1 and Spd2 proteins. Similar to Spd1, Spd2 was degraded in response to HU treatment and this response was completely abolished in CRL4^{Cdt2} defective Δ*ddb1* cells, where the steady state level of Spd2 was also higher than in wild type (Figure 4A). Furthermore, deletion of *spd2* suppressed the elongated cell phenotype and improved the growth rate of CRL4^{Cdt2} defective *Δddb1* cells to approximately the same extent as *spd1* deletion (data not shown). Hence, consistent with the presence of a PIP degron in the protein (Figure 1A), we conclude that Spd2 - like Spd1 - is a target for CRL4^{Cdt2} mediated ubiquitylation

Degradation of Spd2 appeared to be independent of Spd1 and *vice versa* (Figure 4A+C). Deletion of *spd2* apparently caused a modestly elevated Spd1 level in asynchronously growing cells (Figure 4C). Consistent with this, we found that *spd1* mRNA levels were 1.5 fold increased in exponentially growing Δ*spd2* cells compared to wild type (Supplemental Figure S2).

Spd1 becomes degraded as cells enter S phase, because the CRL4 substrate adaptor Cdt2 is controlled by the S phase-specific transcription complex MCB (Liu et al., 2005). We synchronized wild-type cells by centrifugal elutriation and monitored the levels of Spd1 and Spd2 as cells progressed through S phase (Figure 4B). As observed previously (Liu et al., 2003), Spd1 became down-regulated as cells entered S phase, but for Spd2, we could not detect a similar robust reduction.

Spd2 functions in the damage response

CRL4^{Cdt2} defective cells are sensitive to the RNR inhibitor hydroxyurea (HU) and the DNA alkylating agent methyl methane sulphonate (MMS) (Holmberg et al., 2005; Zolezzi et al., 2002),

and this phenotype can be partially suppressed by concomitantly deleting the *spd1* gene, suggesting that accumulation of excess Spd1 protein contributes to the observed drug sensitivity. We therefore investigated whether deletion of the *spd2* gene could also affect the damage sensitivity of $CRL4^{Cdt2}$ defective *Δddb1* cells. Rescue of the MMS sensitivity of Δ*ddb1* occurred to a similar modest extent in both Δ*ddb1* Δ*spd1* and Δ*ddb1* Δ*spd2* double mutants and there was no further suppression in the Δ*ddb1* Δ*spd1* Δ*spd2* triple mutant. However, the observed suppression was too weak to draw firm conclusions on the epistatic relationship between *spd1* and *spd2* (Figure 5A). We also tested for sensitivity to the DSB inducing agent zeocin. Similar to *spd1*, deletion of *spd2* could rescue the sensitivity of *Δddb1* cells. However, deletion of *spd1* on its own conferred almost complete suppression, again making it difficult to evaluate epistasis (Figure 5A).

When deleting *spd2*, the HU sensitivity of Δ*ddb1* cells could be suppressed to almost the same extent as when deleting *spd1*, and when both genes were deleted, we saw increased rescue (Figure 5B). Thus, *spd1* and *spd2* can have both overlapping and separate functions in the damage sensitivity conferred by $CRL4^{Cdt2}$ inactivation.

Spd2 is required for $Cdc22^{R1}$-$Suc22^{R2}$ FRET

When the small and large RNR subunits are tagged with two different fluorescent proteins, a FRET signal can be observed in wild-type cells (Nestoras et al., 2010). The underlying molecular mechanism for this signal is not clear, but since it is absent in cells not expressing Spd1, it presumably represents an Spd1-dependent remodelling of RNR complex architecture that brings the two fluorescent proteins in closer proximity. We analysed whether FRET was also dependent on Spd2 and found that this was indeed the case: in both the nucleus and cytoplasm, the FRET signal was lost in a *Δspd2* strain (Figure 6A+B). Thus, both Spd1 and Spd2 promote the architectural change in RNR structure that is manifested by the FRET signal between $Cdc22^{R1}$ and $Suc22^{R2}$.

Spd2 is not required for Suc22^{R2} nuclear import

Spd1 regulates nuclear import of the small RNR subunit Suc22^{R2} (Liu et al., 2003). In wild-type cells, Suc22^{R2} accumulates in the nucleus, while it becomes largely cytosolic in Δ*spd1* mutant cells, and upon HU-induced degradation of Spd1, Suc22^{R2} redistributes to the cytosol (Liu et al., 2003; Nestoras et al., 2010). Since the Cdc22^{R1} subunit is mainly cytosolic, this nuclear export of Suc22^{R2} has been proposed to cause formation of an increased number of active RNR complexes (Liu et al., 2003; Nielsen, 2003). We found that Suc22^{R2} nuclear localization was lost in Δ*spd1* cells but unchanged in Δ*spd2* cells (Figure 6C). Thus, nuclear import of Suc22^{R2} clearly constitutes an Spd1 function not shared by Spd2.

Spd2 accumulation partially inhibits meiosis

Cells defective in the CRL4^{Cdt2} E3 ubiquitin ligase are unable to undergo meiosis, and this defect can be suppressed by concomitantly deleting the *spd1* gene (Holmberg et al., 2005; Nestoras et al., 2010; Yoshida et al., 2003). We therefore tested the effect of deleting *spd2* on meiotic competence of the CRL4^{Cdt2} mutants Δ*ddb1*, Δ*csn1*, and Δ*cdt2* (Figure 7A). The majority of zygotes of all three homothallic CRL4^{Cdt2} mutants could not develop spores (~80-90%; Figure 7A), consistent with previous data, and these defects were suppressed to almost wild-type levels by deletion of *spd1* (~85-90% asci with 4 spores versus 97% in wild type). In contrast, deleting *spd2* in these CRL4^{Cdt2} mutant backgrounds only partially rescued meiosis. Besides empty zygotes (~50%), asci with two spores (~30%) were predominantly formed (Figure 7A,B). A Δ*ddb1* Δ*spd2* Δ*spd1* triple mutant underwent meiosis as efficiently as a Δ*ddb1* Δ*spd1* double mutant (~90% 4-spored asci for both strains). Hence, Spd2 has an inhibitory function during meiosis. However, in contrast to Spd1, meiosis of the CRL4^{Cdt2} mutants was still partially inhibited in the absence of Spd2.

Spd2 accumulation plays a role in checkpoint activation but does not affect dNTP levels

CRL4^{Cdt2} defective cells rely on activation of the Rad3^{ATR} checkpoint for viability and this phenotype is suppressed by deletion of the *spd1* gene (Holmberg et al., 2005; Liu et al., 2003; Nestoras et al., 2010), suggesting that Spd1 accumulation is the major cause of checkpoint activation. We confirmed that CRL4^{Cdt2} defective Δ*ddb1* and Δ*csn1* cells carrying a temperature sensitive *rad3* allele died at the restrictive temperature, and that their viability was largely restored by elimination of the *spd1* gene (Figure 7C). When deleting *spd2* in *rad3-TS* Δ*ddb1* or *rad3-TS* Δ*csn1* backgrounds, we also observed rescue of viability, albeit only partially (Figure 7C). Simultaneous deletion of *spd1* and *spd2* fully restored viability to a level above the *spd1* deletion, suggesting that accumulation of the two proteins can cause checkpoint activation independently of each other (Figure 7C). Thus, Spd1 is the major CRL4^{Cdt2} target causing Rad3^{ATR} dependency, while the contribution from Spd2 appears to be modest.

Presumably, checkpoint activation triggered by Spd1 accumulation is signalled by replication stress involving single stranded DNA formation caused by RNR inhibition and possibly also by interference with PCNA, the other known interaction partner of Spd1 (Holmberg and Nielsen, 2012; Moss et al., 2010; Salguero et al., 2012; Fleck et al., 2013). We found that Δ*spd2* cells – unlike *Δspd1* cells - did not have elevated dNTP pools (Figure 7D). Hence, the modest checkpoint dependency caused by Spd2 accumulation appears to be unrelated to repression of dNTP pools.

Elevated dNTP pools enhance Δ*spd2*-dependent suppression of CRL4^{Cdt2} defects

The results reported thus far in this paper demonstrate that Spd2 shares some but not all functions with Spd1. In particular, overall cellular dNTP pools appear to be repressed by Spd1 but not by Spd2, and we speculated that this difference may explain why - for certain phenotypes - we

observed a weaker rescue of CRL4^{Cdt2} defective cells when deleting *spd2* as opposed to *spd1*. In other words, Spd1-mediated repression of deoxynucleotide pools may still obscure the effect of deleting *spd2*. To test this hypothesis, we monitored the effect of deleting *spd2* in CRL4^{Cdt2} defective cells that had their dNTP pools up-regulated independently of Spd1. In order to do this, we utilized the *cdc22*^{D57N} mutant, which causes elevated dNTP pools because the dATP feedback inhibition of RNR is abolished (Chabes et al., 2003; Fleck et al., 2013). Importantly, CRL4^{Cdt2} compromised Δ*ddb1 cdc22*^{D57N} cells have higher dNTP levels than wild-type (Fleck et al., 2013). Interestingly, homothallic Δ*ddb1* Δ*spd2 cdc22*^{D57N} triple mutant cells sporulated at a level comparable to Δ*ddb1* Δ*spd1* cells and much better than the corresponding Δ*ddb1* Δ*spd2* and Δ*ddb1 cdc22*^{D57N} double mutant cells (Figure 8A). Similarly, the combination of Δ*spd2* and *cdc22*^{D57N} allowed growth of *rad3-TS* Δ*ddb1* at the restrictive temperature to the same extent as Δ*spd1*, and much better than either Δ*spd2* or *cdc22*^{D57N} alone (Figure 8B). These results confirm that Spd2 shares certain functions with Spd1, and are consistent with a model where these shared functions do not include Spd1's control over dNTP levels.

Discussion

The fission yeast Spd1 protein has attracted considerable interest because of its impact on genome integrity, but its biological function remains enigmatic. Strikingly, most of our knowledge of Spd1 function comes from studies of cells that artificially over-accumulate Spd1 – either through ectopic expression of the gene or via inactivation of its $CRL4^{Cdt2}$ degradation pathway. In general, the phenotypes associated with loss of Spd1 function seem quite harmless to the cell. In fact, elimination of Spd1 often improves growth or survival under conditions that challenge genome integrity.

Spd1 inhibits S phase and becomes degraded when cells embark on DNA synthesis. Its function includes a negative effect on deoxynucleotide formation when DNA replication is not ongoing, but perhaps the protein also plays more dynamic roles in preventing damage to the genome (Holmberg and Nielsen, 2012; Fleck et al., 2013).

In this report we have characterized the Spd1-related protein Spd2. We have shown that Spd2 - similar to Spd1 - is a $CRL4^{Cdt2}$-targeted IDP that inhibits DNA replication and modulates RNR structure. Curiously, Spd2 appears to participate only in a subset of Spd1 controlled processes. It seems to be required neither for nuclear import of RNR R2 nor for repression of deoxynucleotide pool levels. Furthermore, the relationship between Spd1 and Spd2 is complex. Both proteins can inhibit S-phase independently of each other when over-accumulating, but for the architectural remodelling of RNR (as manifested by the FRET assay) they seem to cooperate. According to a recent quantitative expression study, Spd1 and Spd2 are present at similar levels in the cell (respectively, ~14,000 and ~16,000 molecules/cell, Marguerat et al., 2012), so their different behaviour seems to be caused by different functions rather than different concentrations.

$CRL4^{Cdt2}$ defective cells constitutively activate their $Rad3^{ATR}$ checkpoint, presumably because Spd1 reduces dNTP pools and interferes with other so far uncharacterized functions important for

genome integrity (see below). Thus, in accordance with previous reports (Holmberg et al., 2005; Liu et al., 2003; Nestoras et al., 2010), we found that the viability of $CRL4^{Cdt2}$ defective *rad3-TS* cells was restored by deleting the *spd1* gene (Figure 7C). However, deletion of *spd2* only caused an intermediate suppression of viability in this assay. Hence, accumulation of Spd2 appears to make cells much less dependent on the $Rad3^{ATR}$ checkpoint pathway for survival than Spd1 accumulation. Furthermore, since simultaneous deletion of *spd1* and *spd2* caused enhanced suppression (Figure 7C), the two proteins appear to activate the checkpoint independently of each other.

Unlike Spd1, Spd2 is not required for nuclear import of $Suc22^{R2}$. Analogous to the *S. cerevisiae* Dif1 protein, genetic analysis suggests that the Hug domain of Spd1 is required for nuclear import of $Suc22^{R2}$ (Nestoras et al., 2010). The Hug domain is well conserved in Spd2 (Figure 1), so the fact that Spd2 is dispensable for $Suc22^{R2}$ nuclear import suggests that other regions in Spd1 are also needed. Consistent with this, mutant *spd1-m2* (replacing amino acids K5, R6 and V7 with alanines) was reported also to be defective in $Suc22^{R2}$ nuclear import (Nestoras et al., 2010). This region is absent in Spd2 (Figure 1A). The biological relevance of Spd1-mediated nuclear $Suc22^{R2}$ import is not yet known, but genetically this function can be separated from checkpoint activation (Nestoras et al., 2010).

Both Spd1 and Spd2 become degraded in a $CRL4^{Cdt2}$ dependent reaction, when RNR is inhibited by HU (Figure 4A+C). Ubiquitylation of $CRL4^{Cdt2}$ target proteins requires binding to DNA-associated PCNA, so in principle Spd1 and Spd2 should also both be down-regulated when Cdt2 is induced at S phase. However, unlike the situation for Spd1, we did not observed a robust down-regulation of Spd2 during unperturbed S phase (Figure 4B).

While Spd1 on its own appears to control deoxynucleotide pools and $Suc22^{R2}$ nuclear import, it mediates the conformational change in RNR complexes (reflected by the FRET signal) together with Spd2. In our assays for checkpoint dependency and meiotic competence, we found that some

inhibitory function remained in the *Δspd2* CRL4^{Cdt2} mutant backgrounds (Figure 7A+C). We reckoned that this might be due to inhibition of dNTP formation by accumulated Spd1 protein. Hence, we introduced the *cdc22*^{D57N} mutation into these backgrounds. This mutation abolishes the allosteric feedback inhibition of RNR and elevates the dNTP pools to a level well above that obtained by deleting *spd1* (Fleck et al., 2013). Interestingly, on their own both the *cdc22*^{D57N} mutation and *Δspd2* could partially rescue the checkpoint requirement and meiotic defect of CRL4^{Cdt2} mutated cells. However, when combined, we saw a better suppression in both assays, similar to the effect obtained by deleting *spd1* (Figure 8A+B). Therefore, an important conclusion of the present study is that excess Spd1can cause checkpoint activation by both deoxynucleoside dependent and independent mechanisms, and only the latter seems to require Spd2. In accordance with this, we recently reported that Spd1 accumulation can cause checkpoint activation even in cells that have elevated dNTP pools due the *cdc22-D57N* mutation (Fleck et al., 2013).

A key unanswered question is how Spd1 and Spd2 can cause checkpoint activation independently of deoxynucleotide regulation. Currently, the only known mutual Spd1-Spd2 function is the conformational change in RNR architecture manifested by the FRET assay. Hence, a molecular characterization of the RNR FRET phenomenon is highly important for understanding how small IDP proteins like Spd1 and Spd2 regulate genome integrity. Equally important, particularly from a cancer perspective, is the issue of whether this complex yet fascinating group of proteins also exists in human cells.

Materials and Methods

Strains and media

Strain construction and growth media were applied according to standard genetic techniques for *S. pombe* (Moreno et al., 1991). A list of strains used in this study is included as Supplemental Table S1. Δ*spd2* was constructed as follows: A PCR reaction was performed with the pFA6a-kanMX plasmid (Bahler et al., 1998) as template and the primer set ONP687 + ONP688 (GATACTTTTTAATTGTTTTACTTATCCAGGCGCCAGCTGAAGCTTCGTAC + TCGAAAGCTTTATCTTGCTCATTTATTCATGGCCACTAGTGGATCTGATA), two additional PCR reactions were performed with purified genomic *S. pombe* DNA and the primer sets ONP689 + ONP690 (ATGAATAAATGAGCAAGATAAAGCTTTCGA + AGTAACTTTCGACACATTCAAATGGTGT) and ONP691 + ONP692 (CCTGGATAAGTAAAACAATTAAAAAGTATC + ACGACTTGAAGCTTACTCGCTTCTAAAAGG). The three PCR products were used for a fusion PCR with ONP690 + ONP692 and the resulting amplicon was used for transformation of Eg432. G418 resistant clones were selected, positive clones were checked for correct recombination of the PCR product and a resulting strain was designated Eg2806 and used for subsequent studies.

Plasmids for overexpression of Spd1 (pON736) or Spd2 (pON1126) from the thiamine-repressible *nmt1* promoter were obtained by cloning the ORFs into pREP3 (Maundrell, 1990).

FACS

Cells were fixed as described by (Kjaerulff et al., 2005), and stained with Sytox Green (Molecular Probes) as recommended by the manufacturer. Quantification of S phase cells with the aid of the DNA signal width was according to (Knutsen et al., 2011). For each sample, a total of 30,000 cells were counted, and after gating at least 75 % were still present.

Sensitivity assays

5-fold dilution series of the indicated strains were spotted onto YEA plates containing the indicated drugs. Plates were cast 2 days prior to use and kept at room temperature. Pictures were taken after 3 days of incubation at 33°C (or indicated temperature).

Structural analysis

The Spd2 ORF was ligated into a pET11a plasmid and expressed in BL21(DE3) cells grown in 1 L LB media to OD_{600} 0.7-0.8 and induced by 0.01 mM IPTG for 3 hours at 37°C. Purification of Spd1 and Spd2 and structural analyses of Spd2 were performed essentially as in (Nestoras et al., 2010). The far-UV CD spectrum of Spd2 was recorded from 250 to 190 nm on 10 μM Spd2 and 10 mM NaH_2PO_4 (pH 7.4) subtracting the corresponding buffer spectrum. The ^{15}N, ^{1}H-HSQC NMR spectrum was recorded on 277 μM ^{15}N-Spd2, 100 mM NaCl and 10 mM NaH_2PO_4 (pH 7.4) at 10 °C.

Western blots

Cultures were grown to midlog phase at 30°C in YE and 5×10^7 cells were harvested. All samples were TCA extracted and run on 15% SDS-PAGE gels and wet-blotted (300 mA) for 1.5 hours at 4°C. After blocking, membranes were incubated ON at 4°C with the indicated primary antibodies. To study protein levels in response to HU treatment, cultures were grown to midlog phase and 5×10^7 cells were harvested, 20mM HU were added to the remainder of the cultures and after 4 hours, 5×10^7 cells were harvested. To analyse synchronous populations, 6 litres of culture was grown to midlog phase and cells were size sorted by elutriation. The smallest sized cells were collected at a concentration of approx. 2×10^6 cells/ml and incubated at 30°C. 1×10^8 cells were

harvested at each of the indicated time points. Polyclonal rabbit α-Spd1 and α-Spd2 antibodies were raised against *E. coli* purified proteins by Yorkshire Bioscience Limited.

Cell biology

Suc22-GFP localisation assay and FRET analysis of the Cdc22/Suc22 FRET-pair were performed as previously described (Nestoras et al., 2010). For meiotic analysis, h^{90} strains of the indicated genotypes were spotted onto solid sporulation medium at 25°C and after three days the number of spores (0 through 4) in at least 100 individual zygotes/asci were counted.

dNTP pools

dNTP measurement were performed as described (Beck et al., 2012) and the levels were normalized to ATP. For normalization, the dNTP/ATP ratio was set to 1 in the wild type.

Acknowledgements

We thank Jon Halvor Knutsen for advice on FACS quantification, Karin Holm for expert technical assistance, Rasmus Hartmann-Petersen for comments on the manuscript and Iain Hagan and Rasmus Hartmann-Petersen for α-Tubulin antibody.

This work was supported by the Danish Cancer Society (ON), the Danish Research Councils (BBK), the National Institute for Social Care and Health Research – Cancer Genetics Biomedical Research Unit (OF), North West Cancer Research (OF) and AICR project 12-1118 (AMC, BBK).

Figure legends

Figure 1. Spd2 is homologous to Spd1 and other known RNR inhibitors. (A) Comparison of amino acid sequences of Spd1 and Spd2 orthologues of the four *Schizosacchomyces* species *S. pombe* (Spo), *S. cryophilus* (Scr), *S. octosporus* (Soc), and *S. japonicus* (Sja). Residues are highlighted in black and grey when they are identical and similar, respectively, between Spd1 and Spd2 orthologues. Amino acid residues in dark and light blue indicate conservation predominantly in Spd1 orthologues, and in dark and light red predominantly in Spd2 orthologues. The Hug domain (*) and the Spd domain (**) are boxed. Amino acids defining the Spd1 PIP degron (Q-x-x-L-x-x-x-x-x-x-x-R) (Salguero et al., 2012) are marked above the aligned sequences. (B) Alignment of Spd2 with other fungal RNR inhibitors. Identical and similar amino acid residues are highlighted in, respectively, black and grey. Hug, Sml, and Rnr1 domains as defined by (Lee et al., 2008) are boxed. Spd1 and Spd2 share a unique domain close to the C-terminus, which we termed the Spd domain.

Figure 2. Structural properties of Spd2. (A) Spd2 was purified to homogeneity and the electrophoretic mobility was investigated by electrophoresis. Lane 1: Marker, Lane 2: Purified Spd2. (B) A far-UV CD spectrum of purified Spd2 showing a large negative ellipticity with a maximum at 199 nm, suggesting a disordered protein with little or no secondary structure. (C) An NMR spectrum of purified Spd2 showing that only a small dispersion of signals was observed in the ^{1}H- dimension, further suggesting the protein is disordered with no globular fold.

Figure 3. Overexpression of Spd2 inhibits S phase. (A) Overexpressing either Spd1 or Spd2 leads to accumulation of a subset of elongated and aberrant cell shapes. The effect of Spd2 overexpression is not dependent on a functional *spd1*$^{+}$ gene and *vice versa*. Cells were grown to

mid-log phase in minimal media with or without thiamine for 24 hours before pictures were taken. Scale bar represents 6 micrometers. (B) Quantification of FACS analysis of cells overexpressing Spd1 or Spd2. Cell cycle distribution was analysed according to (Knutsen et al., 2011). “S1” represents the fraction of S phase cells with one nucleus, while “S2” represents binucleate cells (as defined by the width of the DNA signal) undergoing replication. When overexpressing either Spd1 or Spd2, the proportion of S phase cells increased, in particular "S1" cells. Representative examples of this quantification method are given in Figure S1.

Figure 4. Spd2 is degraded by $CRL4^{Cdt2}$ during S phase and replication stress. (A) Samples from the indicated strains were harvested before and after 4 hours of growth in the presence of hydroxyurea (HU) and the Spd2 levels were monitored by Western blotting. Spd2 was degraded upon HU-induced replication stress in wild type and *Δspd1* cells, but not in $CRL4^{Cdt2}$-defective *Δddb1* cells. (B) Wild-type cells were synchronised in G2 by centrifugal elutriation and samples were harvested at the indicated time-points. Spd1 and Spd2 levels were monitored by Western blotting. The fraction of S-phase cells (Knutsen et al., 2011) peaked at 50% between 80-120 minutes. Unlike Spd1, Spd2 was not strongly down-regulated at S phase. (C) Samples from the indicated strains were harvested before and after 4 hours of growth in the presence of hydroxyurea (HU) and Spd1 levels were monitored by Western blotting. Spd1 was degraded upon HU-induced replication stress in wild type and *Δspd2* cells, but not in *Δddb1* cells. A slightly elevated abundance of Spd1 was observed in *Δspd2* cells. Tubulin was used as loading control in all three panels. A molecular weight marker was run alongside samples and marker bands are given by size (kDa).

Figure 5. Spd2 has a function similar to Spd1 in the damage response. (A) 5-fold serial dilutions of the indicated strains were spotted onto control plates or plates containing the indicated

concentrations of MMS or zeo (= zeocin, a bleomycin related drug). While the sensitivity of *Δddb1* towards MMS is rescued to the same extend in *Δspd1*, *Δspd2* and *Δspd1 Δspd2* mutants cells, zeo sensitivity is rescued better by *Δspd1* than *Δspd2*. (B) Spot test on plates containing 6 or 8 mM HU. Here, *Δspd1 Δspd2* double mutant cells show better rescue of *Δddb1* than either single mutant.

Figure 6. Deleting *spd2* abolishes RNR FRET, but does not affect Suc22 localisation. (A) In wild-type cells, CFP-tagged $Suc22^{R2}$ and YFP-tagged $Cdc22^{R1}$ give rise to a FRET signal, which is lost when either *spd1* or *spd2* is deleted. (B) The FRET signal is lost in both the nucleus and the cytoplasm of *Δspd2* cells (error bars reflect SD; n=8-10 cells). (C) Suc22-GFP accumulates in the nucleus in wild-type cells. The nuclear localisation was intact in *Δspd2* cells, but was abolished in *Δspd1* and *Δspd1Δspd2* cells. Scale bar represents 6 micrometers.

Figure 7. Deleting *spd2* partially rescues the meiotic defect and checkpoint dependency of $CRL4^{Cdt2}$ defective cells. (A) Homothallic h^{90} cells starved for a nitrogen source go through meiosis, resulting in the formation of 4-spored asci. Shown are the percentages of zygotes/asci with 0-4 spores of the various homothallic strains as indicated. In wild-type cells, close to 100% asci are 4-spored. When components of the $CRL4^{Cdt2}$ pathway were absent (*Δddb1*, *Δcdt2* or *Δcsn1*), meiosis became defective, resulting almost exclusively in asci without spores. When deleting *spd1* in $CRL4^{Cdt2}$ defective cells, the sporulation efficiency was reverted to almost wild-type levels. When *spd2* was deleted in $CRL4^{Cdt2}$ defective cells, the sporulation efficiency was only partially rescued. However, most spore-containing asci had fewer than four spores. (B) Representative images of zygotes/asci of wild type and mutants as indicated. While *Δspd1* restored sporulation efficiency of *Δddb1* cells to almost the wild-type level, *Δddb1 Δspd2* mainly produced empty zygotes and asci with 2 spores. Scale bar represents 6 micrometers. (C) Cells lacking a functional $CRL4^{Cdt2}$ pathway

require a functional checkpoint for viability. 10-fold serial dilutions of the indicated strains were spotted onto YEA and incubated for the indicated number of days. *rad3-TS Δddb1* and *rad3-TS Δcsn1* cells were unable to grow at the restrictive temperature. Deletion of *spd1* largely rescued viability, consistent with (Holmberg et al., 2005). Deletion of *spd2* caused a partial rescue of viability in *rad3-TS Δddb1* and *rad3-TS Δcsn1* backgrounds. Simultaneous deletion of *spd1* and *spd2* caused full rescue, suggesting that accumulation of both Spd1 and Spd2 can contribute to checkpoint activation independently of each other. (D) Cellular dATP/ATP concentrations were measured by a primer extension assay as a measure of regulation of overall dNTP pools. Strains lacking *spd1* had elevated dNTP pools due to deregulation of RNR. However, deleting *spd2* did not cause elevated dATP pools. $P<0.05$ for wt vs. *Δspd1* and wt vs. *Δspd1 Δspd2*.

Figure 8. Combining *Δspd2* with the $cdc22^{D57N}$ mutation rescues *Δddb1* deficiencies to the same extent as deleting *spd1*. (A) Consistent with Figure 7A, *Δspd1* rescued the sporulation deficiency of an h^{90} *Δddb1* strain almost fully. Both *Δspd2* and $cdc22^{D57N}$ rescued the deficiency partially, but when combining *Δspd2* and $cdc22^{D57N}$, the sporulation levels were rescued almost fully. (B) Both *Δspd2* and $cdc22^{D57N}$ rescued the viability of a *rad3-TS Δddb1* strain partially, but when combined, viability was rescued to a similar extent as by *Δspd1*. Note that the plates depicted are the same as shown in Figure 7C.

References

Bahler, J., Wu, J. Q., Longtine, M. S., Shah, N. G., McKenzie, A., 3rd, Steever, A. B., Wach, A., Philippsen, P. and Pringle, J. R. (1998). Heterologous modules for efficient and versatile PCR-based gene targeting in Schizosaccharomyces pombe. *Yeast* 14, 943-51.

Basrai, M. A., Velculescu, V. E., Kinzler, K. W. and Hieter, P. (1999). NORF5/HUG1 is a component of the MEC1-mediated checkpoint response to DNA damage and replication arrest in Saccharomyces cerevisiae. *Molecular and cellular biology* 19, 7041-9.

Beck, H., Nahse-Kumpf, V., Larsen, M. S., O'Hanlon, K. A., Patzke, S., Holmberg, C., Mejlvang, J., Groth, A., Nielsen, O., Syljuasen, R. G. et al. (2012). Cyclin-dependent kinase suppression by WEE1 kinase protects the genome through control of replication initiation and nucleotide consumption. *Mol Cell Biol* 32, 4226-36.

Bester, A. C., Roniger, M., Oren, Y. S., Im, M. M., Sarni, D., Chaoat, M., Bensimon, A., Zamir, G., Shewach, D. S. and Kerem, B. (2011). Nucleotide deficiency promotes genomic instability in early stages of cancer development. *Cell* 145, 435-46.

Chabes, A., Georgieva, B., Domkin, V., Zhao, X., Rothstein, R. and Thelander, L. (2003). Survival of DNA damage in yeast directly depends on increased dNTP levels allowed by relaxed feedback inhibition of ribonucleotide reductase. *Cell* 112, 391-401.

Danielsson, J., Liljedahl, L., Barany-Wallje, E., Sonderby, P., Kristensen, L. H., Martinez-Yamout, M. A., Dyson, H. J., Wright, P. E., Poulsen, F. M., Maler, L. et al. (2008). The intrinsically disordered RNR inhibitor Sml1 is a dynamic dimer. *Biochemistry* 47, 13428-37.

Elledge, S. J., Zhou, Z., Allen, J. B. and Navas, T. A. (1993). DNA damage and cell cycle regulation of ribonucleotide reductase. *Bioessays* 15, 333-9.

Fairman, J. W., Wijerathna, S. R., Ahmad, M. F., Xu, H., Nakano, R., Jha, S., Prendergast, J., Welin, R. M., Flodin, S., Roos, A. et al. (2011). Structural basis for allosteric regulation of human ribonucleotide reductase by nucleotide-induced oligomerization. *Nat Struct Mol Biol* 18, 316-22.

Fleck, O., Vejrup-Hansen, R., Watson, A., Carr, A.M., Nielsen, O. and Holmberg, C. (2013). Spd1 accumulation causes genome instability independently of ribonucleotide reductase activity but functions to protect the genome when deoxynucleotide pools are elevated. *J Cell Sci* 126, 4985-4994.

Hakansson, P., Dahl, L., Chilkova, O., Domkin, V. and Thelander, L. (2006). The Schizosaccharomyces pombe replication inhibitor Spd1 regulates ribonucleotide reductase activity and dNTPs by binding to the large Cdc22 subunit. *J Biol Chem* 281, 1778-83.

Halazonetis, T. D., Gorgoulis, V. G. and Bartek, J. (2008). An oncogene-induced DNA damage model for cancer development. *Science* 319, 1352-5.

Hofer, A., Crona, M., Logan, D. T. and Sjoberg, B. M. (2012). DNA building blocks: keeping control of manufacture. *Crit Rev Biochem Mol Biol* 47, 50-63.

Holmberg, C., Fleck, O., Hansen, H. A., Liu, C., Slaaby, R., Carr, A. M. and Nielsen, O. (2005). Ddb1 controls genome stability and meiosis in fission yeast. *Genes Dev* 19, 853-62.

Holmberg, C. and Nielsen, O. (2012). Replication: DNA building block synthesis on demand. *Curr Biol* 22, R271-2.

Kjaerulff, S., Lautrup-Larsen, I., Truelsen, S., Pedersen, M. and Nielsen, O. (2005). Constitutive activation of the fission yeast pheromone-responsive pathway induces ectopic meiosis and reveals ste11 as a mitogen-activated protein kinase target. *Mol Cell Biol* 25, 2045-59.

Knutsen, J. H., Rein, I. D., Rothe, C., Stokke, T., Grallert, B. and Boye, E. (2011). Cell-cycle analysis of fission yeast cells by flow cytometry. *PLoS One* 6, e17175.

Lee, Y. D., Wang, J., Stubbe, J. and Elledge, S. J. (2008). Dif1 is a DNA-damage-regulated facilitator of nuclear import for ribonucleotide reductase. *Mol Cell* 32, 70-80.

Liu, C., Poitelea, M., Watson, A., Yoshida, S. H., Shimoda, C., Holmberg, C., Nielsen, O. and Carr, A. M. (2005). Transactivation of Schizosaccharomyces pombe cdt2+ stimulates a Pcu4-Ddb1-CSN ubiquitin ligase. *Embo J* 24, 3940-51.

Liu, C., Powell, K. A., Mundt, K., Wu, L., Carr, A. M. and Caspari, T. (2003). Cop9/signalosome subunits and Pcu4 regulate ribonucleotide reductase by both checkpoint-dependent and -independent mechanisms. *Genes Dev* 17, 1130-40.

Marguerat, S., Schmidt, A., Codlin, S., Chen, W., Aebersold, R. and Bähler J. (2012). Quantitative analysis of fission yeast transcriptomes and proteomes in proliferating and quiescent cells. *Cell* 151, 671-683.

Maundrell, K. (1990). nmt1 of fission yeast. A highly transcribed gene completely repressed by thiamine. *J Biol Chem* 265, 10857-64.

Moreno, S., Klar, A. and Nurse, P. (1991). Molecular genetic analysis of fission yeast Schizosaccharomyces pombe. *Methods Enzymol* 194, 795-823.

Moss, J., Tinline-Purvis, H., Walker, C. A., Folkes, L. K., Stratford, M. R., Hayles, J., Hoe, K. L., Kim, D. U., Park, H. O., Kearsey, S. E. et al. (2010). Break-induced ATR and Ddb1-Cul4(Cdt)(2) ubiquitin ligase-dependent nucleotide synthesis promotes homologous recombination repair in fission yeast. *Genes Dev* 24, 2705-16.

Nestoras, K., Mohammed, A. H., Schreurs, A. S., Fleck, O., Watson, A. T., Poitelea, M., O'Shea, C., Chahwan, C., Holmberg, C., Kragelund, B. B. et al. (2010). Regulation of ribonucleotide reductase by Spd1 involves multiple mechanisms. *Genes Dev* 24, 1145-59.

Nielsen, O. (2003). COP9 signalosome: a provider of DNA building blocks. *Curr Biol* 13, R565-7.

Nordlund, P. and Reichard, P. (2006). Ribonucleotide reductases. *Annu Rev Biochem* 75, 681-706.

Reichard, P. (2010). Ribonucleotide reductases: substrate specificity by allostery. *Biochem Biophys Res Commun* 396, 19-23.

Rhind, N., Chen, Z., Yassour, M., Thompson, D. A., Haas, B. J., Habib, N., Wapinski, I., Roy, S., Lin, M. F., Heiman, D. I. et al. (2011). Comparative functional genomics of the fission yeasts. *Science* 332, 930-6.

Salguero, I., Guarino, E., Shepherd, M. E., Deegan, T. D., Havens, C. G., MacNeill, S. A., Walter, J. C. and Kearsey, S. E. (2012). Ribonucleotide reductase activity is coupled to DNA synthesis via proliferating cell nuclear antigen. *Curr Biol* 22, 720-6.

Tompa, P. (2002). Intrinsically unstructured proteins. *Trends Biochem Sci* 27, 527-33.

Uchiki, T., Dice, L. T., Hettich, R. L. and Dealwis, C. (2004). Identification of phosphorylation sites on the yeast ribonucleotide reductase inhibitor Sml1. *J Biol Chem* 279, 11293-303.

Weinberg, G., Ullman, B. and Martin, D. W., Jr. (1981). Mutator phenotypes in mammalian cell mutants with distinct biochemical defects and abnormal deoxyribonucleoside triphosphate pools. *Proc Natl Acad Sci U S A* 78, 2447-51.

Woollard, A., Basi, G. and Nurse, P. (1996). A novel S phase inhibitor in fission yeast. *Embo J* 15, 4603-12.

Wu, X. and Huang, M. (2008). Dif1 controls subcellular localization of ribonucleotide reductase by mediating nuclear import of the R2 subunit. *Mol Cell Biol* 28, 7156-67.

Yoshida, S. H., Al-Amodi, H., Nakamura, T., McInerny, C. J. and Shimoda, C. (2003). The Schizosaccharomyces pombe cdt2(+) gene, a target of G1-S phase-specific transcription factor complex DSC1, is required for mitotic and premeiotic DNA replication. *Genetics* 164, 881-93.

Zhao, X., Georgieva, B., Chabes, A., Domkin, V., Ippel, J. H., Schleucher, J., Wijmenga, S., Thelander, L. and Rothstein, R. (2000). Mutational and structural analyses of the ribonucleotide reductase inhibitor Sml1 define its Rnr1 interaction domain whose inactivation allows suppression of mec1 and rad53 lethality. *Mol Cell Biol* 20, 9076-83.

Zhao, X. and Rothstein, R. (2002). The Dun1 checkpoint kinase phosphorylates and regulates the ribonucleotide reductase inhibitor Sml1. *Proc Natl Acad Sci U S A* 99, 3746-51.

Zolezzi, F., Fuss, J., Uzawa, S. and Linn, S. (2002). Characterization of a Schizosaccharomyces pombe strain deleted for a sequence homologue of the human damaged DNA binding 1 (DDB1) gene. *J Biol Chem* 277, 41183-91.

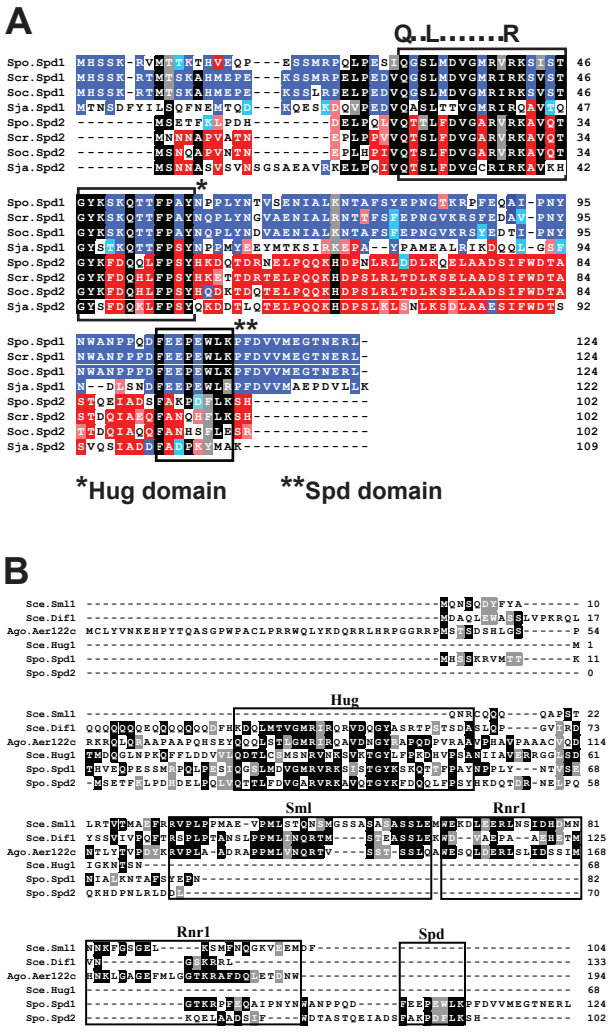

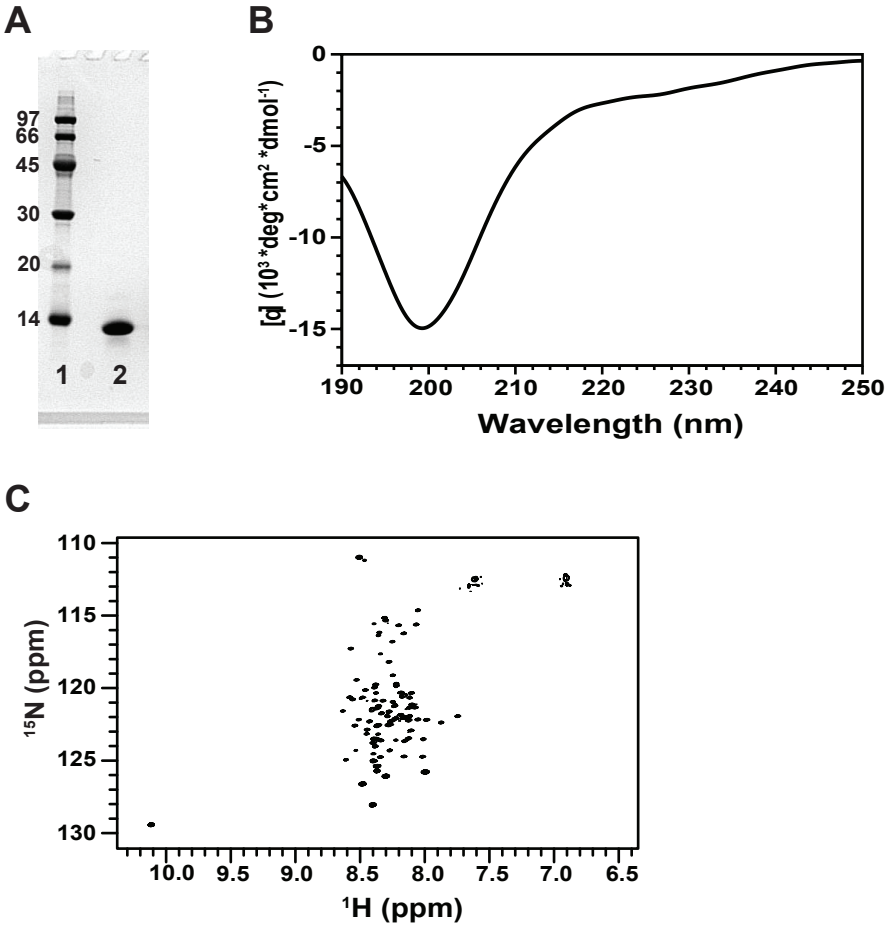

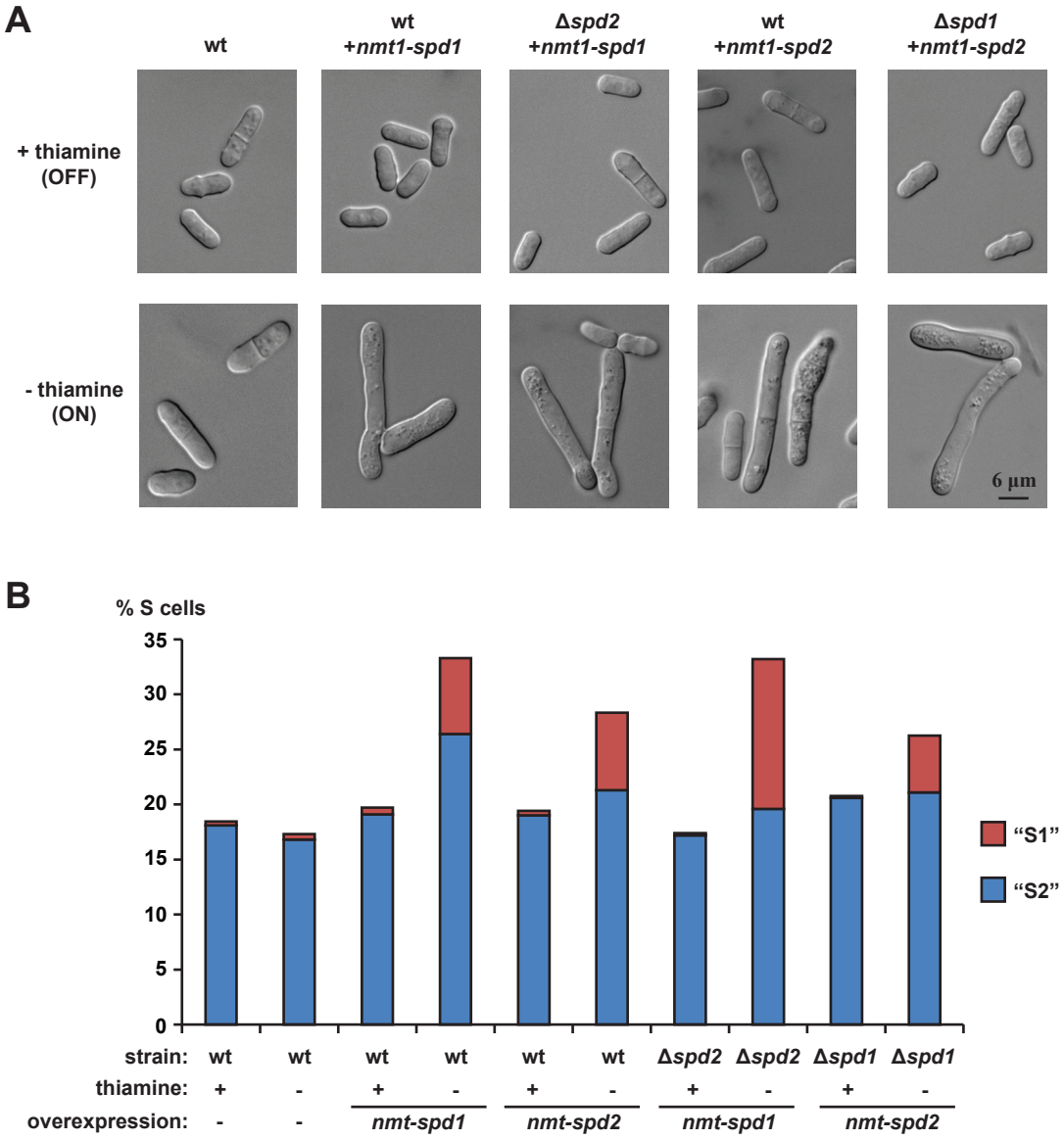

Figure 3